

Acoustic Imaging in Turbulent Media with the Spatial Bispectrum

John A. Tague and Y.D. Cheng
Department of Electrical and Computer Engineering
Ohio University
Athens, Ohio 45701-2979
tague@hammer.ece.ohiou.edu

Abstract

We introduce a new array processing system that performs high resolution imaging in turbulent ocean media. It exploits information contained in higher order spatial spectra and images to a resolution which is limited by the array aperture rather than the medium. Precise *a priori* knowledge of the turbulence's spatial coherence structure is not needed. Furthermore, the signal processing is straightforward to implement, the system is self-calibrating, and the computational demands are reasonable. We have conducted initial tests of the imager and present representative results.

1. Introduction

In this paper, we study a new imaging system that performs high resolution imaging in turbulent underwater media. The problem under consideration is posed as follows. An extended acoustic source reflects or radiates narrowband energy with known center wavelength. A sensor array, located some distance from the object, collects measurements of the acoustic wavefield produced by the object. The problem is to process the data and image the object with aperture-limited resolution.

Acoustic imaging can be performed by measuring the object's reflected or radiated power with a sensor array.¹⁻³ The image is formed by sweeping its beam through a region of interest and estimating the beamformer's output power as a function of position. In any kind of imaging system, wavefield coherence across the array's aperture is essential in order to resolve details to the aperture's Rayleigh limit. But conventional imaging systems, such as the Bartlett or Capon methods, can not work to their full potential in turbulent ocean media. Turbulence produces random phase variations across the wavefield, and when the array is longer than the wavefield's coherence length, its resolving power can be reduced significantly.⁴ This

blurs the image, reduces its contrast, and hinders the ability to identify the object.

We therefore propose a new imaging system using higher order spectral analysis of spatial domain data.⁵ It resolves features to the array's Rayleigh limit, even in turbulent media. We attack the problem by first decomposing the Bartlett image into a Fourier series. All subsequent processing is performed on the Fourier series coefficients, which contain the information required to synthesize the image. The image's Rayleigh-limited magnitude spectrum is extracted from second order moments of the Fourier coefficients. The image's Rayleigh-limited phase spectrum is extracted from third order moments of the Fourier coefficients. The estimates are then combined to synthesize the image.

We pose the problem in Section 2 and describe the imager in Section 3. We present an example of its performance in Section 4, and our conclusions appear in Section 5. In this paper, $*$, H , and T denote complex conjugate, Hermitian transpose, and transpose respectively. The expression $E\{\cdot\}$ denotes the mathematical expectation operator.

2. Problem Formulation

The object radiates narrowband acoustic energy, modeled as a zero mean, wide-sense stationary random process with center wavelength λ . In addition, we will assume that the object radiates incoherently; in other words, signals originating from different locations are statistically uncorrelated. This assumption simplifies the signal processing. We make no other assumptions regarding its structure; that is, parametric models of the object are not used.

We will model the turbulence-free ocean as an infinite, homogeneous medium. Therefore, in the absence of turbulence, we will assume that acoustic energy from a distant point source propagates in plane waves.

The turbulence introduces random phase variations into wavefield measurements.^{4,9} Random magnitude variations will be neglected. Ocean turbulence effects can be quantified by statistical moments; those of interest here are its coherence time and coherence length.⁹ We will assume that the coherence time is known and is constant across the array aperture. We need the coherence time in order to set the system integration time correctly.

We do not need to know the spatial properties of the turbulence. Spatial phase fluctuations will be cancelled out by averaging higher order moments of the image. Therefore, the array processor does not require *a priori* knowledge of its spatial coherence properties, nor does it use it if available.

A line array constructed from N identical transducers will be used to measure the wavefield. The spacing between adjacent sensors is d . The output of the i th sensor at time t , in complex envelope form, is $x_i(t)$. We sample the sensor outputs and collect L measurements from each. We next show how to process these data and image the object with aperture-limited resolution.

3. The Technique

A. Reformulate the Bartlett estimator

The Bartlett estimator forms an image by sweeping a beam through a predetermined search sector and measuring power as a function of bearing θ .^{2,3} The resulting image $P(\theta)$ can be represented by the quadratic form

$$P(\theta) = \mathbf{e}^H(\theta) \mathbf{R} \mathbf{e}(\theta), \quad (1)$$

where \mathbf{R} is the array correlation matrix and

$$\mathbf{e}(\theta) = [1 \ e^{-j2\pi d \sin \theta / \lambda} \ \dots \ e^{-j(N-1)2\pi d \sin \theta / \lambda}]^T \quad (2)$$

steers the beam to θ degrees with respect to array boresight.

Let us now look at Eq. (1) from a different perspective. Since the object is an incoherent radiator, \mathbf{R} is a Toeplitz matrix; therefore, it can be reformulated into

$$P(\theta) = \sum_{k=-(N-1)}^{N-1} I(k) e^{jk2\pi d \sin \theta / \lambda}. \quad (3)$$

Eq. (3) is the Fourier series representation of $P(\theta)$. The k th coefficient $I(k) = (N - |k|)r_k$, where $r_k = E\{x_m(t)x_{m-k}^*(t)\}$ is the correlation between sensors m and $m - k$. The image's magnitude spectrum is denoted $\{|I(k)|\}$ and its phase spectrum is denoted $\{\phi(k)\}$.

In practice, the $\{I(k)\}$ sequence is unknown and must be estimated by correlating sensor output time series data. For example, if there were no turbulence, we could estimate $I(2)$ by computing

$$\hat{I}(2) = \sum_{m=3}^N \frac{1}{L} \sum_{t=1}^L x_m(t) x_{m-2}^*(t). \quad (4)$$

But the preceding procedure will not work properly in a turbulent medium. Ocean turbulence decorrelates the wavefield across the aperture; therefore, the spatial coherence required to estimate $\{I(k)\}$ directly from sensor data is lost. In particular, the high frequency components of $P(\theta)$ are affected the most, especially if the turbulence coherence length is much less than the array aperture. Under these conditions, $E\{\hat{I}(k)\} = 0$ for large values of k . We conclude that the high frequency information, essential for Rayleigh-limited resolution, is not available in the first order statistics of $\{I(k)\}$. Beginning in the next section, we therefore derive a new coherent processing method that uses second and third order statistics of $\{I(k)\}$.

B. Parse the sensor output time series

The first step is to parse the sensor outputs into Q consecutive segments containing M samples each. Therefore, $L = Q \times M$. The segment width is less than or equal to the turbulence coherence time. This ensures that within each segment, the turbulence phase variation on the m th sensor is approximately fixed. All sensor outputs are segmented the same way.

The next step is to cross-correlate array data within each data segment. Let $x_m^{(q)}(t_l)$ denote the l th measurement of the output of sensor m within frame Q . Then we correlate sensor time series data as follows:

$$\hat{r}_{m \rightarrow m-k}^{(q)} = \frac{1}{M} \sum_{l=1}^M x_m^{(q)}(t_l) x_{m-k}^{(q)*}(t_l), \quad (5)$$

for $k+1 \leq m \leq N$ and $1 \leq q \leq Q$. The $m \rightarrow m-k$ notation means that we cross correlate the output of sensor m with the output of sensor $m-k$. Each such correlation represents an estimate of r_k corrupted by turbulence phase shifts. If $\hat{r}_k^{(q)}$ is the turbulence free estimate of r_k , and $\theta_m^{(q)}$ and $\theta_{m-k}^{(q)}$ are the turbulence-induced shifts on sensors m and $m-k$ respectively, then $\hat{r}_{m \rightarrow m-k}^{(q)} = \exp\{j(\theta_m^{(q)} - \theta_{m-k}^{(q)})\} \hat{r}_k^{(q)}$. The phase shifts are approximately constant because we average well within the turbulence coherence time. An N -element array gives $N-k$ estimates of r_k per data segment.

C. Estimate the image magnitude spectrum

The third step is to estimate the image's magnitude spectrum. The idea is based on the observation that turbulence phases cancel out in the second order symmetry⁸

$$\hat{r}_k^{(q)} \hat{r}_{-k}^{(q)} = |\hat{r}_k^{(q)}|^2. \quad (6)$$

The turbulence phases also cancel in $|\hat{r}_k^{(q)}|$; hence, for convenience, we propose averaging these quantities.

We propose the following procedure. First, compute $|\hat{r}_{m \rightarrow m-k}^{(q)}|$ for $k+1 \leq m \leq N$ within each segment. Then, within segment q , compute

$$\sum_{m=k+1}^N |\hat{r}_{m \rightarrow m-k}^{(q)}| \quad (7)$$

and average over the Q segments:

$$|\widehat{I}(k)| = \frac{1}{Q} \sum_{q=1}^Q \sum_{m=k+1}^N |\hat{r}_{m \rightarrow m-k}^{(q)}|. \quad (8)$$

All phase information is removed, including the random phase shifts as well as the image phases; what remains is Rayleigh-limited magnitude information. The phase information must be obtained another way.

D. Estimate the image bispectrum

Rayleigh-limited image phase information can be extracted from the image bispectrum, defined by the triple product^{5,7}

$$I(k_1)I(k_2)I(-k_1 - k_2) = B_3(k_1, k_2). \quad (9)$$

It can be proven that we need only estimate $B_3(k_1, k_2)$ on its principal domain, a wedge-shaped grid of points on the (k_1, k_2) plane. The principal domain contains all of the information needed to estimate the image phases.

We will estimate $B_3(k_1, k_2)$ as follows. Within segment q , compute

$$\widehat{B}_3^{(q)}(k_1, k_2) = \widehat{I}^{(q)}(k_1) \widehat{I}^{(q)}(k_2) \widehat{I}^{(q)}(-k_1 - k_2), \quad (10)$$

where

$$\widehat{I}^{(q)}(k_1) = \sum_{m=k_1+1}^N \hat{r}_{m \rightarrow m-k_1}^{(q)} \quad (11)$$

and

$$\widehat{I}^{(q)}(-k_1 - k_2) = \sum_{m=1}^{N-k_1-k_2} \hat{r}_{m \rightarrow m+k_1+k_2}^{(q)} \quad (12)$$

Next, average the Q estimates:

$$\widehat{B}_3(k_1, k_2) = \frac{1}{Q} \sum_{q=1}^Q \widehat{B}_3^{(q)}(k_1, k_2). \quad (13)$$

Why does the bispectrum work? First, recognize that we can decompose the phase of $I(k)$ into the sum $\phi(k) = k\phi_D + \phi_S(k)$. The first term is linear in k ; it carries direction of arrival information. The second term is nonlinear in k , and carries object structure information. Now suppose that we estimate $B_3(3, 1)$ from a four element array. Within the q th data segment,

$$\widehat{B}_3(2, 1) = \widehat{I}^{(q)}(2) \widehat{I}^{(q)}(1) \widehat{I}^{(q)}(-3). \quad (14)$$

The array provides three estimates of r_1 , two estimates of r_2 , and one estimate of r_{-3} . Substitute them into equation (14):

$$\widehat{B}_3(2, 1) = (\hat{r}_{3 \rightarrow 1}^{(q)} + \hat{r}_{4 \rightarrow 2}^{(q)}) (\hat{r}_{2 \rightarrow 1}^{(q)} + \hat{r}_{3 \rightarrow 2}^{(q)} + \hat{r}_{4 \rightarrow 3}^{(q)}) (\hat{r}_{1 \rightarrow 4}^{(q)}). \quad (15)$$

Now consider the phase of the product $\hat{r}_{2 \rightarrow 1}^{(q)} \hat{r}_{4 \rightarrow 2}^{(q)} \hat{r}_{1 \rightarrow 4}^{(q)}$:

$$\begin{aligned} & \widehat{\phi}_D + \widehat{\phi}_S(1) - \theta_1^{(q)} + \theta_2^{(q)} + 2\widehat{\phi}_D + \widehat{\phi}_S(2) - \theta_2^{(q)} + \theta_4^{(q)} \\ & - \widehat{\phi}_D + \widehat{\phi}_S(-3) - \theta_4^{(q)} + \theta_1^{(q)} \\ & = \widehat{\phi}_S(1) + \widehat{\phi}_S(2) + \widehat{\phi}_S(-3). \end{aligned} \quad (16)$$

The turbulence phases $\theta_1^{(q)}$, $\theta_2^{(q)}$, and $\theta_4^{(q)}$ cancel out in this "phase closed" triple product.²¹ So does ϕ_D , which carries the object's bearing information. However, the phases which carry the high resolution structural information, $\widehat{\phi}_S(1)$, $\widehat{\phi}_S(2)$, and $\widehat{\phi}_S(-3)$ do not cancel. They can be extracted from $\widehat{B}_3(k_1, k_2)$ using the recursion presented in the next section.

Why do we average over Q data segments? When we compute $\widehat{B}_3^{(q)}(k_1, k_2)$, the result is the sum of $(N - k_1)(N - k_2)(N - k_1 - k_2)$ terms. Each term is the product of three estimated cross correlation coefficients; the phases close in $N - k_1 - k_2$ of the triple products. The phases in the remaining triple products do not close, and these phases retain the random turbulence phases. In the averaging process, the phase closed triple products add coherently and the other triple products add incoherently. Therefore, averaging over independent frames raises the signal-to-noise ratio. Precise image phase estimates can then be extracted from the estimated bispectra phases.

E. Reconstruct the image phase spectrum

The final step is to unravel the phase spectrum of $P(\theta)$ from the bispectrum.¹⁰ Let us demonstrate how the procedure works with an example. Suppose we process a seven element array and we want $\hat{\phi}(4)$. Let $\hat{\beta}(k_1, k_2)$ denote the phase of $\hat{B}_3(k_1, k_2)$. The image phases are related to the bispectrum phases by the following recursive formula:

$$\hat{\phi}(p+q) = \hat{\phi}(p) + \hat{\phi}(q) - \hat{\beta}(p, q). \quad (17)$$

A seven element array provides two estimates of $\hat{\phi}(4)$. When $(p, q) = (2, 2)$, then

$$\hat{\phi}(4) = 4\hat{\phi}_1 - 2\hat{\beta}(1, 1) - \hat{\beta}(2, 2). \quad (18)$$

When $(p, q) = (3, 1)$, then

$$\hat{\phi}(4) = 4\hat{\phi}_1 - \hat{\beta}(1, 1) - \hat{\beta}(2, 2) - \hat{\beta}(3, 1). \quad (19)$$

Notice that $4\hat{\phi}(1)$ appears in both equations. In general, it can be proven that $k\hat{\phi}(1)$ appears in all equations used to estimate $\phi(k)$. This implies that $\phi(1)$ can not be determined from the bispectrum; it represents the linear phase information lost in the closure phases. The bispectrum provides high resolution image structure phase information, but the arrival direction information is lost. We will set $\hat{\phi}(1) = 0$ to simplify phase reconstruction. The estimate for $\phi_S(4)$ is computed by averaging $\exp(j\cdot)$ terms. In summary, the following recursion is used to compute $\hat{\phi}(p)$:

$$\begin{aligned} \exp\{j\hat{\phi}(p)\} = \\ c \cdot \sum_{0 < q \leq p/2} \exp\{j(\hat{\phi}(q) + \hat{\phi}(p-q) - \hat{\beta}(p-q, q))\}, \end{aligned} \quad (20)$$

where c is an appropriate scaling coefficient, $\hat{\phi}(0) = 0$, $\hat{\phi}(1) = 0$, and $2 \leq p \leq N - 1$. Note that we average exponential functions of $\hat{\phi}(p)$ rather than phases directly because the phases are only determined up to modulo 2π . This concludes the estimation process; the image is reconstructed by substituting the magnitude and phase spectrum estimates into Eq. 3.

4. An Example

We have tested the imaging system on several prototype problems. In the following examples, the object was modeled by two uncorrelated, unit power point sources at +10 and +30 degrees in the far field.

We modeled ocean turbulence by introducing spatially correlated random phase shifts into the measurements with coherence length 10λ . The phase shift on any given sensor was modeled by a random variable uniformly distributed between $-\pi$ and $+\pi$ and was fixed within a given segment. The phase shifts were uncorrelated between time segments. We process simulated data from a discrete line array with 21 sensors spaced sensors $d = \lambda/2$ meters apart. The data set was made up of $Q = 150$ independent segments containing $M = 200$ array snapshots per segment.

Fig. 1 is the baseline image. We found that the magnitude spectrum estimate was very close to the true magnitude spectrum; they are not displayed. Figs. 2 and 3 are the true and reconstructed phase spectra. We now find significant differences between them because the linear portion of $\{\phi(k)\}$ is not reconstructed correctly.

Fig. 4 shows the reconstructed image and the Bartlett image. In terms of resolution and contrast, the Bartlett image quality is poor; however, the peaks appear at the correct bearings. The reconstructed image manifests good resolution and contrast quality, but as expected, the peaks do not appear in the proper locations. Notice that the angular spacing between peaks is slightly less than 20° . The reconstructed phase spectrum differs from the true phase spectrum by an undetermined linear function of k plus estimation errors. But the exponent of Eq. (3) is linear in $\sin \theta$ not θ ; this accounts for the slight distortion.

5. Conclusions

Higher order spectrum analysis can be used to image objects through ocean turbulence. The resolution of the reconstructed image is limited by the array's aperture rather than the spatial coherence properties of the medium. The spatial bispectrum is the most important component of the signal processing. Precise, low variance bispectrum estimates are needed for high quality images, and in this sense, we trade off resolution against data requirements. Although the direction of arrival information is lost in the bispectrum estimation process the object's structural information is not. We have tested the imager and we conclude that it is a viable and interesting new technique.

Acknowledgments

We thank Drs. Edmund J. Sullivan and Dennis Goodman for their ideas and interest in this work.

References

1. Hua Lee and Glen Wade, **Modern Acoustic Imaging**, IEEE Press, 1986.
2. D.H. Johnson and D.E. Dudgeon, **Array Signal Processing: Concepts and Techniques**, Prentice-Hall, 1993.
3. S.L. Marple, Jr., **Digital Spectral Analysis with Applications**, Prentice-Hall, 1987.
4. W.M. Carey and W.B. Mosley, "Space-Time Processing, Environmental-Acoustic Effects," **IEEE Trans. Oceanic Engineering**, Vol. 16, No. 3, pp. 285-300, July 1991.
5. A.W. Lohmann, "Triple correlations," **Proceedings of the IEEE**, Vol. 72, No. 7, pp. 889-901, July 1984.
6. F. Roddier, "Interferometric imaging in optical astronomy," **Phy. Repts.**, Vol. 170, No. 2, 1988.
7. T.W. Lawrence *et. al.*, "Extended-image reconstruction through horizontal path turbulence using bispectral speckle interferometry," **Optical Engineering**, Vol. 31, No. 3, pp. 627-636, March 1992.
8. A.W. Lohmann, "Speckle masking in astronomy: triple correlation theory and applications," **Applied Optics**, Vol. 22, No. 24, pp. 4028-4037, 15 December 1983.
9. S.M. Flatte, **Sound Transmission Through A Fluctuating Ocean**, Cambridge University Press, 1979.
10. H. Bartelt *et. al.*, "Phase and amplitude recovery from bispectra," **Applied Optics**, Vol. 23, No. 18, pp. 3121-3129, 15 September 1984.

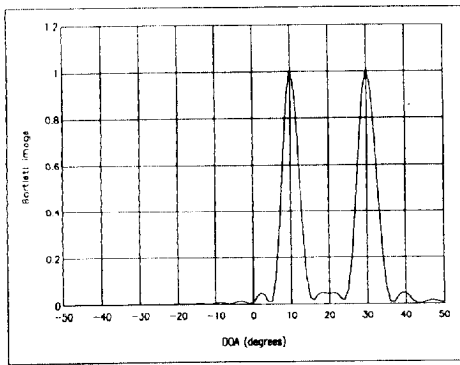


Figure 1

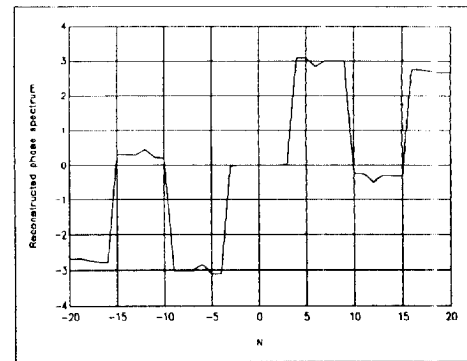


Figure 3

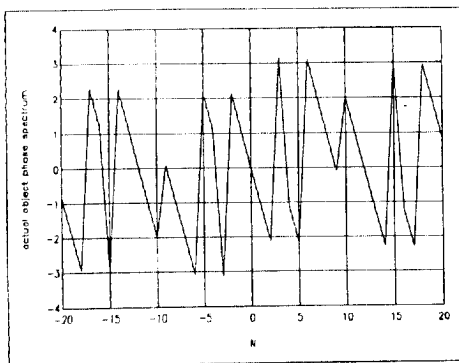


Figure 2

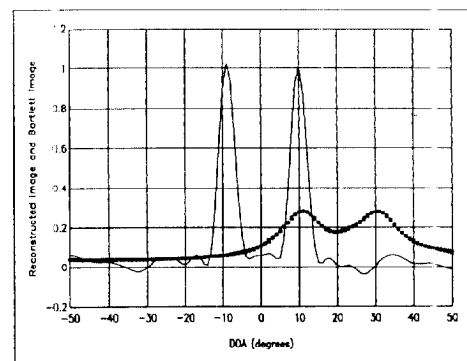


Figure 4